Journal of Materials Chemistry C

RSC Publishing

PAPER

View Article Online
View Journal | View Issue

Cite this: J. Mater. Chem. C, 2013, 1, 2548

The tunable electrical properties of graphene nano-bridges†

Peng Zhou,* Hongqiang Wei, Qingqing Sun,* Pengfei Wang, Shijin Ding, Anquan Jiang and David Wei Zhang

Received 24th January 2013
Accepted 18th February 2013

DOI: 10.1039/c3tc30145a

www.rsc.org/MaterialsC

Reduced graphene oxide nano-bridges and tunable electrical transport properties of reduced graphene oxide based transistors are achieved by using tip-based nanolithography. The polarity dependence of the reduction is revealed with a threshold reduction bias of −6 V on the nano-scale tip. The best carrier mobilities up to now for holes and for electrons in reduced-graphene-oxide-based nano-scale transistors are about 5.6 $cm^2 V^{-1} s^{-1}$ and 3.2 $cm^2 V^{-1} s^{-1}$ at room temperature. Moreover, the tunable output and transport properties have been realized for the first time by the controlled nano-tip electrochemical reaction with different reduction nano-tip biases. These tunable electrical properties of graphene based transistors will be extended to develop various novel optoelectronic and microelectronic applications. It opens a possible way to mass production of a graphene oxide based device, representing a significant step forward for electrical applications.

Introduction

Tailoring graphene for various applications has been studied intensively to break the zero bandgap limitation of its intrinsic monolayer, since it has the highest carrier mobility and saturation velocity among presently known semiconductors.[1,2] In the literature, bilayer graphene under gated voltage control with a tunable bandgap up to 250 meV has been achieved,[3] and tailoring the graphene into a nanoribbon graphene transistor device with a cut-off frequency of 50 GHz (ref. 4) with a low on/off ratio has been shown. However, these processing steps need an ultra-low temperature, expensive state-of-art fabrication technologies or an extremely precise control, which bring great challenges for mass production. Especially, residual photoresist and electron-beam lithography, and plasma etching during processing can either introduce undesired impurities or break the chemical bonds in the graphene lattices, which leads to a significant degradation of its properties. The recent development of reduced graphene oxide (RGO)[5] as an attractive alternative to the graphene, formed *via* hydroiodic acid reductant[6] instead of the traditional reducing reagent in the Staudenmaier method can minimize defects and other unwanted functional groups to preserve the high electrical quality. RGO can be used as a graphene supplement with less residual functional groups and structural defects, which broadens the RGO-based transistor applications even in highly sensitive gas sensors[7] and mechanical resonators with figures of merit surpassing those of graphene-based resonators.[8]

In nature, graphene oxide (GO) is an insulator[9,10] because of the hydroxyl, carboxyl, carbonyl and epoxide functional groups present on the basal surface or edge, and becomes a semiconductor as it is reduced back to graphene.[11,12] Therefore, GO can be used as a native oxide to build a novel all-graphene-based field transistor.[13]

Experimental

The fabrication of GO films was carried out by vacuum filtration of the dispersion as described in ESI section S1† using a mixed cellulose ester membrane filter, pressed against the surface of the SiO_2/Si wafer and bare Si wafer, respectively, and finally dried. Atomic force microscopy (AFM) and conductive atomic force microscopy (CAFM) measurements were performed under ambient conditions, using a MultiMode VIII instrument equipped with a Nanoscope V controller. Contact-mode Pt/Ir-coated silicon cantilevers (Veeco PIT-200) were employed for current mapping and local GO reduction. Standard dynamic-mode cantilevers (Veeco TESP) were used for tapping-mode (intermittent-contact) imaging. During CAFM measurement, a force of 12 nN was maintained. The nano-tip was constantly virtually grounded. Bias voltages were applied to the sample. A scan rate of 1.0 Hz and sample line of 256 were used for both CAFM imaging and GO reduction.

Results and discussion

To resolve the critical zero-bandgap problem in graphene based devices, we developed a nano-tip based nanolithography

ASIC & System State Key Lab, School of Microelectronics, Fudan University, Shanghai 200433, China. E-mail: pengzhou@fudan.edu.cn; qqsun@fudan.edu.cn

† Electronic supplementary information (ESI) available. See DOI: 10.1039/c3tc30145a

approach to arbitrarily fabricate all-graphene-based devices based on graphene oxide with tunable electrical transport properties. The tunable band-gap of the graphene based transistor will attract intensive attention as pioneering research work in band-gap tuning studies. Meanwhile, the tunable electrical transport properties of the graphene related device can explore many applications such as flexible electronics, photo-detectors and biosensors. By using nano-tip based CAFM lithography, we fabricated a graphene nano-bridge under the tip field only through a controlled electrochemical reduction of the graphene oxide. The reduction of this graphene oxide shows polarity dependence on the bias applied voltage, providing the experimental evidence of the intrinsic mechanism of electrochemical reaction. With the arbitrarily configured graphene nano-bridges using AFM tip, we fabricated a back-gated graphene transistor and showed a typical gate-controlled characteristic. Meanwhile, the best hole and electron mobilities for reduced graphene oxide based nano-scale transistor are calculated to be about 5.6 and 3.2 $cm^2 V^{-1} s^{-1}$ under different back-gated voltages at room temperature, respectively. The experimental results are encouraging because we not only show the possibility to tune the bandgap in a reduced graphene oxide based device, but also test the functionality of the graphene oxide as native oxides for transistors, representing a significant step toward to all-carbon-based electrical applications.

Fabrication of GO films was carried out by vacuum filtration of the dispersion using a mixed cellulose ester membrane filter and spin-coated onto Si substrates (see ESI S1†). The layer number of graphene oxide on the substrate is 7 layers determined from spectroscopic ellipsometry using Lorentz model fitting (see ESI S2†). The other functional groups to degrade graphene oxide properties are mostly –COOH and –OH, and were inspected by X-ray photoelectron spectroscopy (XPS).

The schematic diagram of a graphene nano-bridge device fabricated into the 7-layer GO/Si structure by the nano-tip electrical reduction process is illustrated in Fig. 1a. The reduction was performed by applying a variable voltage between the Pt/Ir coated CAFM tip with a radius of 10 nm and the substrate in the contact mode, then we scanned the tip over the film surface with a constant force. Nano-tip based CAFM lithography emerges as a novel way to nano-pattern the devices in different environments including air and organic solvents,[14,15] especially for graphene, because of its high resolution in the lateral size control and ability of *in situ* electrical characterization and modification.[16] Fig. 1b shows the current image in a 5×5 μm^2 region with a voltage of +3 V applied to the bottom electrode to detect the pristine GO film surface conductivity. The current keeps at a very low level of about 0.01 nA with excellent uniformity in the whole region. To investigate the electrically induced GO reduction, we firstly wrote a 2×2 μm^2 square with a higher positive voltage of +8 V on GO within the above center region, and then mapped the current across the region at a fixed voltage of +3 V again, as shown in Fig. 1c. Obviously, the current in the region is still so small as to be negligible. For comparison, an opposite polarity of −8 V bias was applied in other regions.

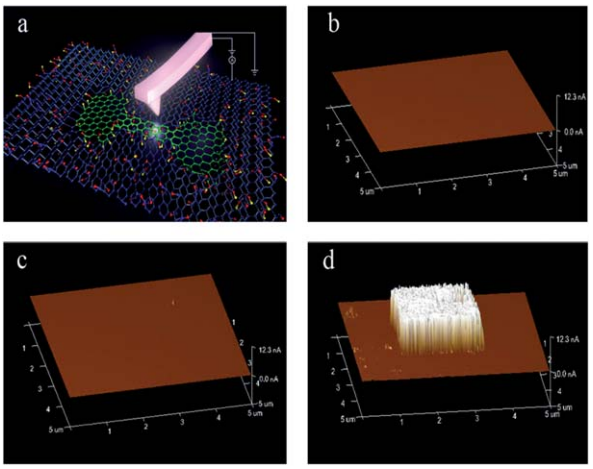

Fig. 1 The polarity dependence of nano-tip based electrical reduction of GO. (a) A schematic diagram of a graphene nano-bridge device which was fabricated on 7-layer GO and the CAFM system configuration; (b) 3-D current mapping of pristine GO film using a probe bias of +3 V in a 5 μm × 5 μm region; (c) 3-D current mapping of a 2 μm × 2 μm scanned region under +8 V applied bias in detected 5 μm × 5 μm GO region; (d) 3-D current mapping of a 2 μm × 2 μm scanned region under −8 V applied sample bias in detected 5 μm × 5 μm GO region. It indicates that current appears only when negative sample bias was applied.

Unexpectedly, the mapping current quickly increases over 3 orders of magnitude, as shown in Fig. 1d, beyond the maximum detection limitation of 12.3 nA in this measurement, implying the possibility of the electrochemical reduction of the highly insulating GO layer into a good semiconductor. However, this only occurs at negative voltages, which are not observed in the opposite positive fields.

The polarity dependence of electrochemical reduction is very helpful to understand the intrinsic mechanism of the field induced chemical reaction between the AFM tip and the film. Firstly, we repeatedly checked if the AFM tip scanning could damage the film surface. If the mechanical damage occurs between the scanning tip and 7-layer GO (~7 nm), the high leakage current can also be achieved *via* electrical short paths. To rule out this possibility, the topographies of the 5×5 μm^2 film before and after tip scanning at −8 V were compared. There is almost no topographical difference shown in Fig. 2a and b, respectively. Therefore, the nano-tip based electrical scan is non-destructive to the film.

To clarify the possible electrochemical reduction of the GO film at negative voltages (RGO), Raman spectra were collected in the reduced region to identify the composition change, as shown in Fig. 2c. Raman spectroscopy is a widely used non-destructive tool for the characterization of graphene materials,[17] and disturbed conjugated and double carbon–carbon bonds can be sensitively reflected from the variation of Raman peak intensities pertinent to the graphene lattice information. Raman spectra were measured using an exciting laser wavelength of 514 nm on GO before and after −8 V poling, as shown in Fig. 2c. The G-peak and 2D-peak shifted from 1600 cm^{-1}, 2682 cm^{-1} to 1588 cm^{-1}, 2690 cm^{-1}, respectively, mostly due to the transition of the bond hybridization from sp^3 to sp^2 in the reduced graphene oxide. The value of the I_D/I_G ratio in Raman

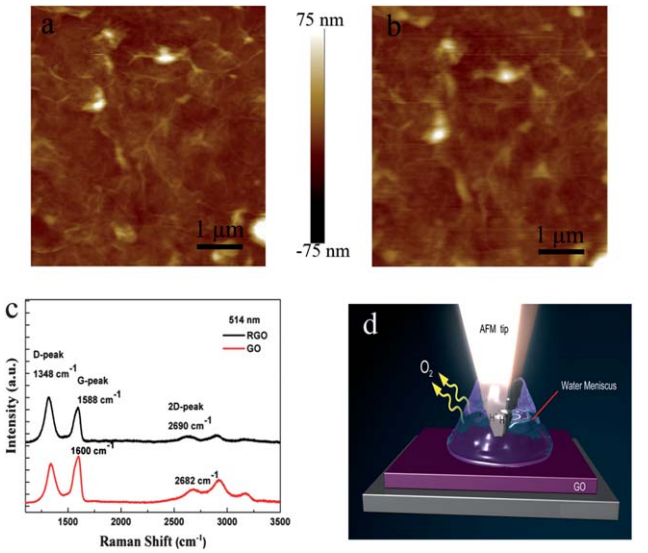

Fig. 2 Topographic images of a detected 5 μm × 5 μm GO film region (a) before and (b) after scanned by reduction bias which were obtained by AFM in tapping mode. No mechanical damage was observed. (c) Raman spectra of pristine GO (red line) and nano-tip electrical reduced GO (black line) with −8 V sample bias. The I_D/I_G ratio increases after the reduction process. (d) A schematic diagram of the mechanism for nano-tip based electrochemical reduction of graphene oxide. When negative sample bias voltage is applied to the GO, hydrogen ions are generated, which play an essential role in the reduction of GO.

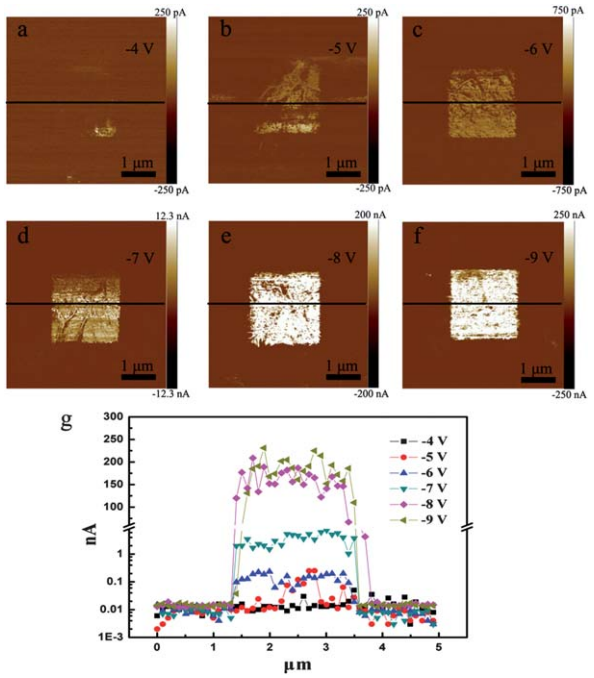

Fig. 3 Current mapping results of 2 μm × 2 μm regions scanned using (a) −4 V, (b) −5 V, (c) −6 V, (d) −7 V, (e)−8 V and (f) −9 V as probe bias *via* +3 V sample bias, respectively. It can be observed that with the increase of reduction bias, the detected currents become more obvious and denser and reach saturation when −8 V and −9 V reduction bias were applied. (g) Currents along the selected black lines across the 2 μm × 2 μm regions scanned with different reduction bias voltages as shown in (a)–(f). Abrupt rising and falling of currents here means accurate position control in this nano-tip-based reduction lithography.

spectra of RGO (1.26) depicted in Fig. 2c indicates fewer sp^3 bonds than in GO (0.87) which reveals a partial GO reduction with enhanced sp^2 clusters created through removal of oxygen during electrochemical reaction.[18] Therefore, it is concluded that GO is apparently reduced to the graphene after −8 V scanning from the Raman examinations. The mechanism of this polarity dependence correlated to the electrochemical reduction involves into hydrogen ions on the GO surface. The schematic diagram of this mechanism is illustrated in Fig. 2d. When a negative voltage is applied to GO, a high electrical field converges between the tip and GO surface, and electrons are injected from sample which induces the hydrogen ions.[19,20] Thus electrochemical reduction of GO happens. Holes rather than electrons are injected when the field direction is reversed, in a lack of electron assisted hydrogen ion generation, the reduction of GO cannot occur at positive voltages. It is also found that the electrochemical reduction of graphene oxide becomes easier with an increase in the local environmental humidity.

The electrochemical reduction depends on the electrical field strength, besides the field polarity. Fig. 3 shows the current mapping after −4 V, −5 V, −6 V, −7 V, −8 V and −9 V AFM tip reduction. There is almost no evidence of the reduction when the sample bias is above −4 V except a small accident spot of about 0.01 nA at a location on the lower right bottom of the 2 × 2 μm^2 region in Fig. 3a. When the bias decreases to −5 V, the GO reduction, though weak, begins to occur (Fig. 3b) since the current amplitude increases a little. At −6 V, the process accelerates as shown in Fig. 3c, where the current increases up to 0.1 nA in most parts of the scanned region. The reduction at −4 and −6 V was repeated in ten other regions which show no exception. A significant increase of the current suddenly occurs at voltages below −7 V. Therefore, the threshold voltage for the occurrence of a massive electrochemical reduction of a 7-layer graphene oxide seems to be −6 ± 0.5 V. The current quickly increases up to the several nA order in Fig. 3d and reaches a maximum value of about 200 nA at −8 V in Fig. 3e. Then the current remains saturated with the further reduction of the poling voltage to −9 V in Fig. 3f. Meanwhile, we can accurately position a 2 × 2 μm^2 poling region within a 5 × 5 μm^2 area, as shown in Fig. 3g. The sharpness of mapping currents along the black line across the edges at 1.5 μm and 3.5 μm away from the left panel side shows the accurate control of the reduction position in this nano-tip-based process at various voltages from Fig. 3a–f. The current increment is obvious, though the current is not very uniform along the line because of the GO inhomogeneity over such a large area.

The thin layer graphene oxide with controllable electrochemical reduction shows a tunable bandgap, and it has been proved using the other chemical reduction method (see in ESI S3†). It is believed that the *in situ* tailored bandgap using tip-based nanolithography is more convenient at variable voltages than other pure chemical methods, though they can both change the bandgap. The controllable reduction of GO in a nano-meter scale provides tunable electrical characteristic of RGO based transistor. Since the nano-tip based electrochemical

reduction has an accurate position control, the graphene nano-bridge is made using this tip-based nanolithography, as shown in Fig. 4a, with the width as short as around 400 nm and the length as long as 10.5 μm. Here the −7 V and −8 V reduction voltages were used in the fabrication process to induce different electrical transport properties. We used this graphene nano-bridge to make a back-gated graphene transistor for investigation of the output current–voltage (*I–V*) characteristics, where electrochemically reduced GO was used as channel materials. A schematic diagram of this novel device is shown in Fig. 4b (the device fabrication process and measurement method can be found in ESI S4†). Fig. 4c shows the back-gated voltage control of an *I–V* curve at a −7 V reduction bias. The channel current reaches 2.25 μA under a 20 V drain voltage, and the current slightly increases with increasing gate voltage from −10 to −40 V. In comparison, the current quickly increases up to 30 μA when the reduction sample bias is −8 V as Fig. 4d shown, *i.e.*, an order of magnitude larger in the channel current. This enhancement can be attributed to the deep reduction level of GO by a reduced reduction bias. The transfer characteristic of this graphene nano-bridge using −7 V and −8 V reduction bias was both investigated with a source–drain voltage of 20 V as shown in Fig. 4e. From the transfer characteristics curve, we calculated the hole and electron mobility to be equal to about 5.6 $cm^2 V^{-1} s^{-1}$ and 3.2 $cm^2 V^{-1} s^{-1}$ at room temperature, respectively (the calculation detail see ESI S5†). The nano-tip based lithography using electrochemical reduction demonstrates a novel constructed RGO device in graphene oxide plain.

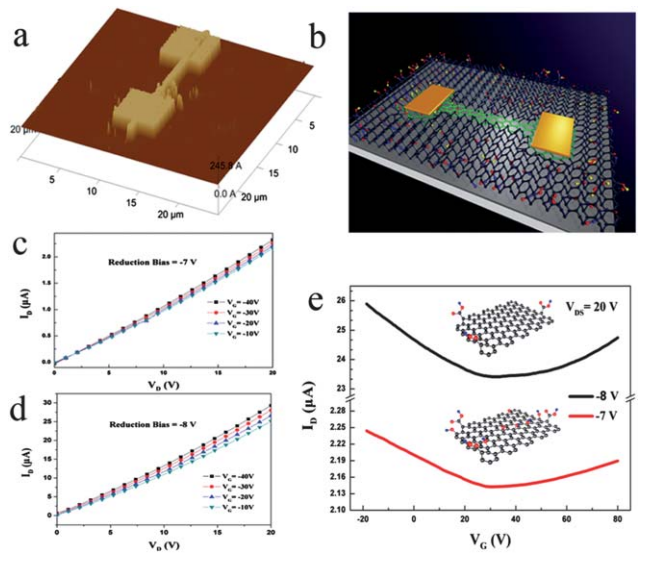

Fig. 4 (a) Graphene nano-bridge construction is realized by nano-tip based nanolithography. (b) A schematic diagram of a back-gated transistor with reduced GO used as the channel material which was patterned by nano-tip based nanolithography with different reduction bias voltages. The back-gated voltage control I_D–V_D curves with RGO channel reduced by (c) −7 V and (d) −8 V reduction bias, respectively. Four different negative gate voltages varying by steps of 10 V were applied. (e) Transfer characteristics of the devices measured with RGO channels reduced by −7 V (red line) and (d) −8 V (black line) reduction bias. Source–drain voltage of 20 V was applied.

Conclusions

In summary, we constructed a reduced graphene oxide structure with a width as short as around 400 nm and the length as long as 10.5 μm in the graphene oxide plane using nano-tip based lithography from contact atomic force microscopy and configured it into a back gated transistor successfully. The polarity dependence of the reduction was revealed with a threshold reduction bias of −6 V. The tunable electrical transport properties of reduced graphene oxide based transistors controlled by the different reduction bias are firstly achieved using tip-based nanolithography, where the best carrier mobility up to now for holes and for electrons in reduced graphene oxide based nano-scale transistors is about 5.6 $cm^2 V^{-1} s^{-1}$ and 3.2 $cm^2 V^{-1} s^{-1}$ at room temperature. These tunable electrical properties of graphene based transistors will be extended to develop various novel optoelectronic and microelectronic applications based on the mass manufacturable graphene oxide layer with tunable band-gap and this promising lithography method to tailor the nano-structure freely.

Acknowledgements

We are thankful for the financial support of NSFC (61076114), Innovation Program of Shanghai Municipal Education Commission, SRFDP (20100071120027), and National Science and Technology Major Project (2011ZX02707).

Notes and references

1 K. S. Novoselov, V. I. Falko, L. Colombo, P. R. Gellert, M. G. Schwab and K. Kim, *Nature*, 2012, **490**, 192–200.
2 Y. B. Zhang, Y. W. Tan, H. L. Stormer and P. Kim, *Nature*, 2005, **438**, 201–204.
3 Y. B. Zhang, T. T. Tang, C. Girit, Z. Hao, M. C. Matin, A. Zettl, M. F. Crommie, Y. R. Shen and F. Wang, *Nature*, 2009, **459**, 820–823.
4 L. Liao, J. W. Bai, R. Cheng, H. L. Zhou, L. X. Liu, Y. Liu, Y. Huang and X. F. Duan, *Nano Lett.*, 2011, **12**, 2653–2657.
5 S. F. Pei and H. M. Cheng, *Carbon*, 2012, **50**, 3210–3228.
6 I. K. Moon, J. Lee, R. S. Ruoff and H. Lee, Reduced graphene oxide by chemical graphitization, *Nat. Commun.*, 2010, **1**, 73.
7 J. T. Robinson, F. K. Perkins, E. S. Snow, Z. Q. Wei and P. E. Sheehan, Reduced graphene oxide molecular sensors, *Nano Lett.*, 2008, **8**, 3137–3140.
8 J. T. Robinson, M. Zalalutdinov, J. W. Baldwin, E. S. Snow, Z. Q. Wei, P. E. Sheehan and B. H. Houston, Wafer-scale reduced graphene oxide films for nanomechanical devices, *Nano Lett.*, 2008, **8**, 3441–3445.
9 S. Stankovich, D. A. Dikin, G. H. B. Dommett, K. M. Kohlhaas, E. J. Zimney, E. A. Stach, R. D. Piner, S. T. Nguyen and R. S. Ruoff, Graphene-based composite materials, *Nature*, 2006, **442**, 282–286.
10 G. Wang, B. Wang, J. Park, J. Yang, X. Shen and J. Yao, Synthesis of enhanced hydrophilic graphene oxide nanosheets by a solvothermal method, *Carbon*, 2009, **47**, 68–72.

11 G. Eda, C. Mattevi, H. Yamaguchi, H. Kim and M. J. Chhowalla, Insulator to semimetal transition in graphene oxide, *J. Phys. Chem. C*, 2009, **113**, 15768–15771.

12 X. S. Wu, M. Sprinkle, X. Li, F. Ming, C. Berger and W. A. Heer, Epitaxial-graphene/graphene-oxide junction: an essential step towards epitaxial graphene electronics, *Phys. Rev. Lett.*, 2008, **101**, 026801.

13 S. K. Lee, H. Y. Jang, S. Jang, E. Choi, B. H. Hong, J. Lee, S. Park and J. H. Ahn, All graphene-based thin film transistors on flexible plastic substrates, *Nano Lett.*, 2012, **12**, 3472–3476.

14 R. Garcia, R. V. Martinez and J. Martinez, Nano-chemistry and scanning probe nanolithographies, *Chem. Soc. Rev.*, 2006, **35**, 29–38.

15 C. R. Kinser, M. J. Schmitz and M. C. Hersam, Conductive atomic force microscope nanopatterning of hydrogen-passivated silicon in inert organic solvents, *Nano Lett.*, 2005, **5**, 91–95.

16 R. K. Puddy, P. H. Scard, D. Tyndall, M. R. Connolly, C. G. Smith, G. A. C. Jones, A. Lombardo, A. C. Ferrari and M. R. Buitelaar, Atomic force microscope nanolithography of graphene: cuts, pseudocuts, and tip current measurements, *Appl. Phys. Lett.*, 2011, **98**, 133120.

17 A. C. Ferrari, J. C. Meyer, V. Scardaci, C. Casiraghi, M. F. Mauri, S. Piscanec, D. Jiang, K. S. Novoselov, S. Roth and A. K. Geim, Raman spectrum of graphene and graphene layers, *Phys. Rev. Lett.*, 2006, **97**, 187401.

18 A. C. Ferrari and J. Robertson, Interpretation of Raman spectra of disordered and amorphous carbon, *Phys. Rev. B: Condens. Matter Mater. Phys.*, 2000, **61**, 14095–14107.

19 M. Zhou, Y. Wang, Y. Zhai, J. Zhai, W. Ren, F. Wang and S. Dong, Controlled synthesis of large-area and patterned electrochemically reduced graphene oxide films, *Chem.–Eur. J.*, 2009, **15**, 6116–6120.

20 S. Masubuchi, M. Arai and T. Machida, Atomic force microscopy based tunable local anodic oxidation of graphene, *Nano Lett.*, 2011, **11**, 4542–4546.

